Science Advances
AAAS

Supplementary Materials for

Channel width modulates the permeability of DNA origami–based nuclear pore mimics

Qingzhou Feng *et al.*

Corresponding author: Chenxiang Lin, chenxiang.lin@yale.edu

Sci. Adv. **10**, eadq8773 (2024)
DOI: 10.1126/sciadv.adq8773

The PDF file includes:

Other Supplementary Material for this manuscript includes the following:

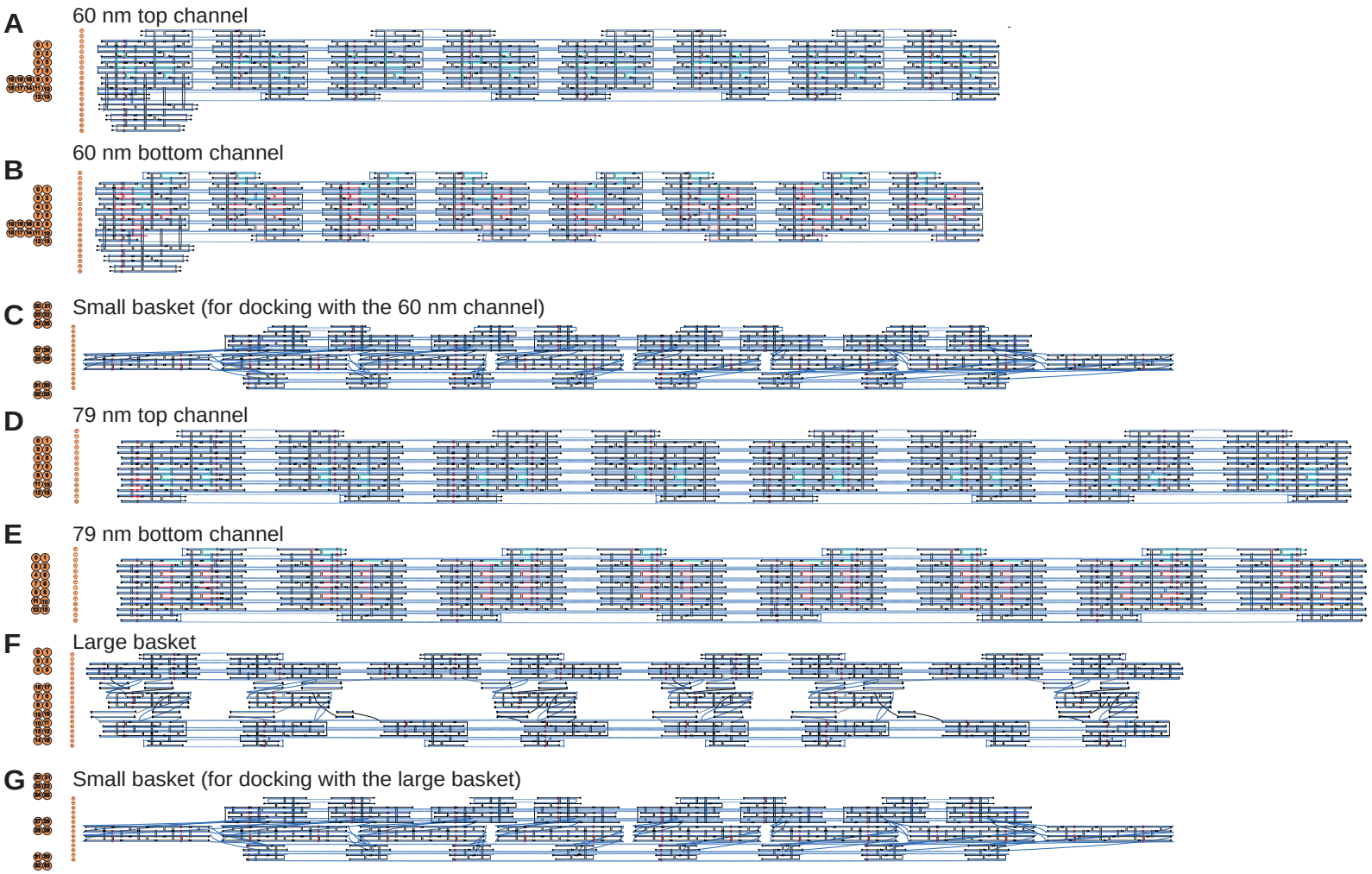

Figure S1. DNA origami designs shown as caDNAno diagrams.
(A)–(G): individual DNA origami structures for building NuPODs. For (A), (B), (D) and (E), the 3'-ends of the green and red staple strands represent handle positions for Nup62 and Nup153, respectively. (A)&(B) have the same main structure but different sticky-end designs on their docking interfaces. So are (C)&(G) and (D)&(E).

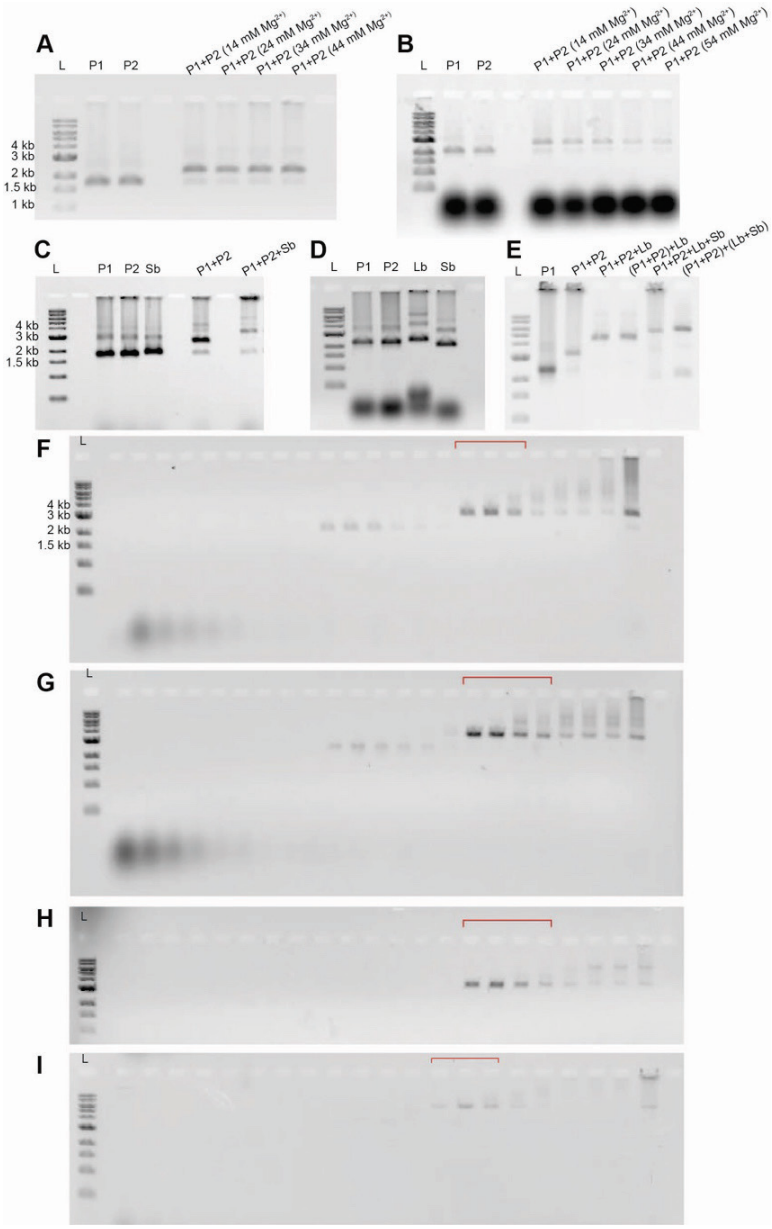

Figure S2. DNA origami assembly and purification.

(A) Assembly of the open-ended 60-nm channel at various Mg^{2+} concentrations characterized by agarose gel electrophoresis. **(B)** Assembly of the open-ended 79-nm channel at various Mg^{2+} concentrations characterized by agarose gel electrophoresis. **(C)** Assembly of the capped 60-nm channel characterized by agarose gel electrophoresis. **(D)** The 79-nm NuPOD components characterized by agarose gel electrophoresis. **(E)** Assembly of the capped 79-nm channel characterized by agarose gel electrophoresis. L: 1kb DNA ladder; P1: top channel; P2: bottom channel; Lb: large basket; Sb: small basket. Parentheses denote pre-assembled components. **(F)** Open-ended 60-nm channel purified by rate-zonal centrifugation. **(G)** Open-ended 79-nm channel purified by rate-zonal centrifugation. **(H)** Capped 60-nm channel purified by rate-zonal centrifugation. **(I)** Capped 79-nm channel purified by rate-zonal centrifugation. For **(F)–(I),** fractions 5–27 are resolved by agarose gel electrophoresis (lighter fractions on the left), and the collected fractions containing the correctly assembled structures are denoted by red brackets.

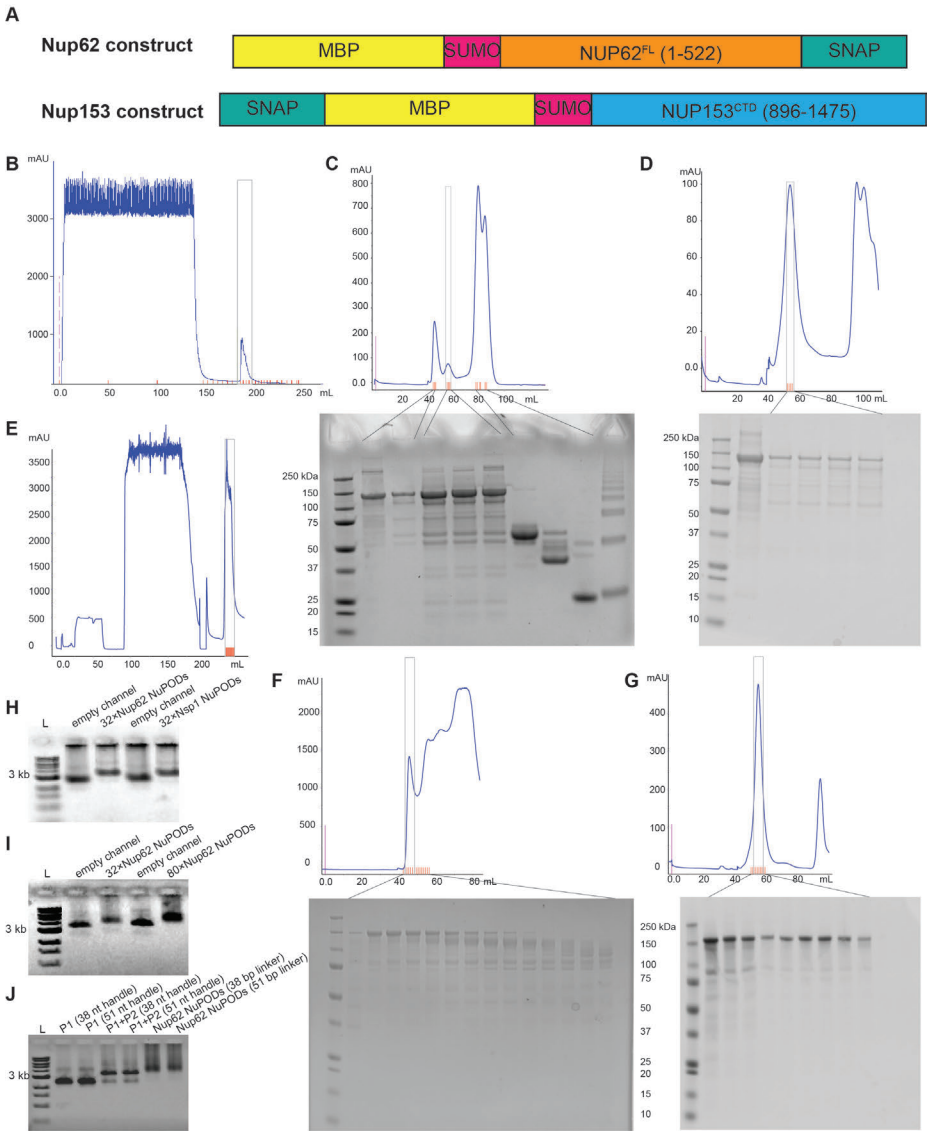

Figure S3. Preparation of nups, nup-DNA conjugates, and NuPODs.

(A) Schematics of the Nup62 and Nup153 constructs used in this work. **(B)** Purification of Nup62 by MBP affinity chromatography. Elusions in the grey box are collected for further purification by size-exclusion chromatography (SEC). **(C)** SEC purification of Nup62. Boxed fractions are collected for DNA conjugation. **(D)** SEC purification of DNA-conjugated Nup62. Boxed fractions are collected for NuPOD assembly. **(E)** Purification of Nup153 by His affinity chromatography. Elusions in the grey box are collected for further purification by size-exclusion chromatography (SEC). **(F)** SEC purification of Nup153. Boxed fractions are collected for DNA conjugation. **(G)** SEC purification of DNA-conjugated Nup153. Boxed fractions are collected for NuPOD assembly. Selected fractions in **(C), (D), (F),** and **(G)** are characterized by SDS-PAGE. **(H)** Agarose gel (0.05% SDS) electrophoresis (SDS-AGE) showing the band shifts of open-ended 60-nm Nup62 and Nsp1 NuPODs compared with empty DNA channel dimers. This experiment was repeated twice (technical replicates) with similar results. **(I)** SDS-AGE showing the band shifts of open-ended 79-nm NuPODs with different Nup62 copy numbers compared with empty DNA channel dimers. **(J)** SDS-AGE gel showing the band shifts of 79-nm Nup62 NuPODs with different handle lengths compared with empty DNA channel monomers (P1) and dimers (P1+P2).

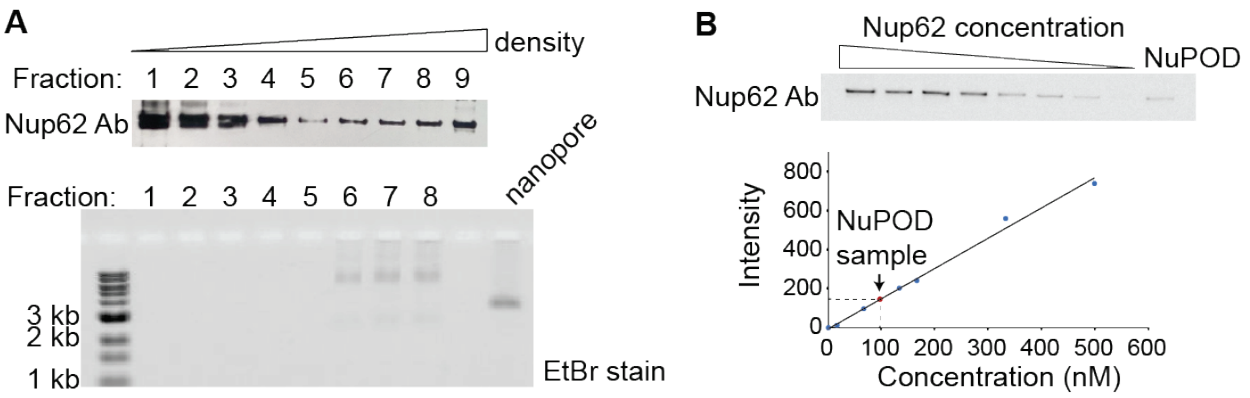

Figure S4. Measuring the Nup62 copy number inside a NuPOD.

(A) Rate-zonal centrifugation separates free Nup62 from NuPODs. Top: Fractions recovered after rate-zonal centrifugation of unpurified Nup62 NuPODs, characterized by SDS-PAGE/western blot (detected using Nup62 antibody); Bottom: The first 8 fractions characterized by SDS-agarose gel electrophoresis (SAS-AGE) and stained by ethidium bromide. Lighter fractions are shown on the left. **(B)** Western blot for measuring Nup62 concentration in the purified NuPOD, a mixture of fractions 6–8 shown in **(A)**. Top, SDS-PAGE/western blot (detected using Nup62 antibody) of purified Nup62 (the first 8 lanes) and Nup62 NuPOD (the right most lane). Bottom: A plot showing western blot band intensity (y) against known Nup62 concentration (x), with linear regression (solid line) yielding $y=1.547x-3.604$ ($R^2=0.99$). The red dot represents the NuPOD band intensity and the corresponding Nup62 concentration (94.3 nM). Given the NuPOD concentration (3.05 nM, estimated by band intensity comparison with empty nanopore in SDS-AGE), we estimated ~31 copies of Nup62 in one NuPOD on average.

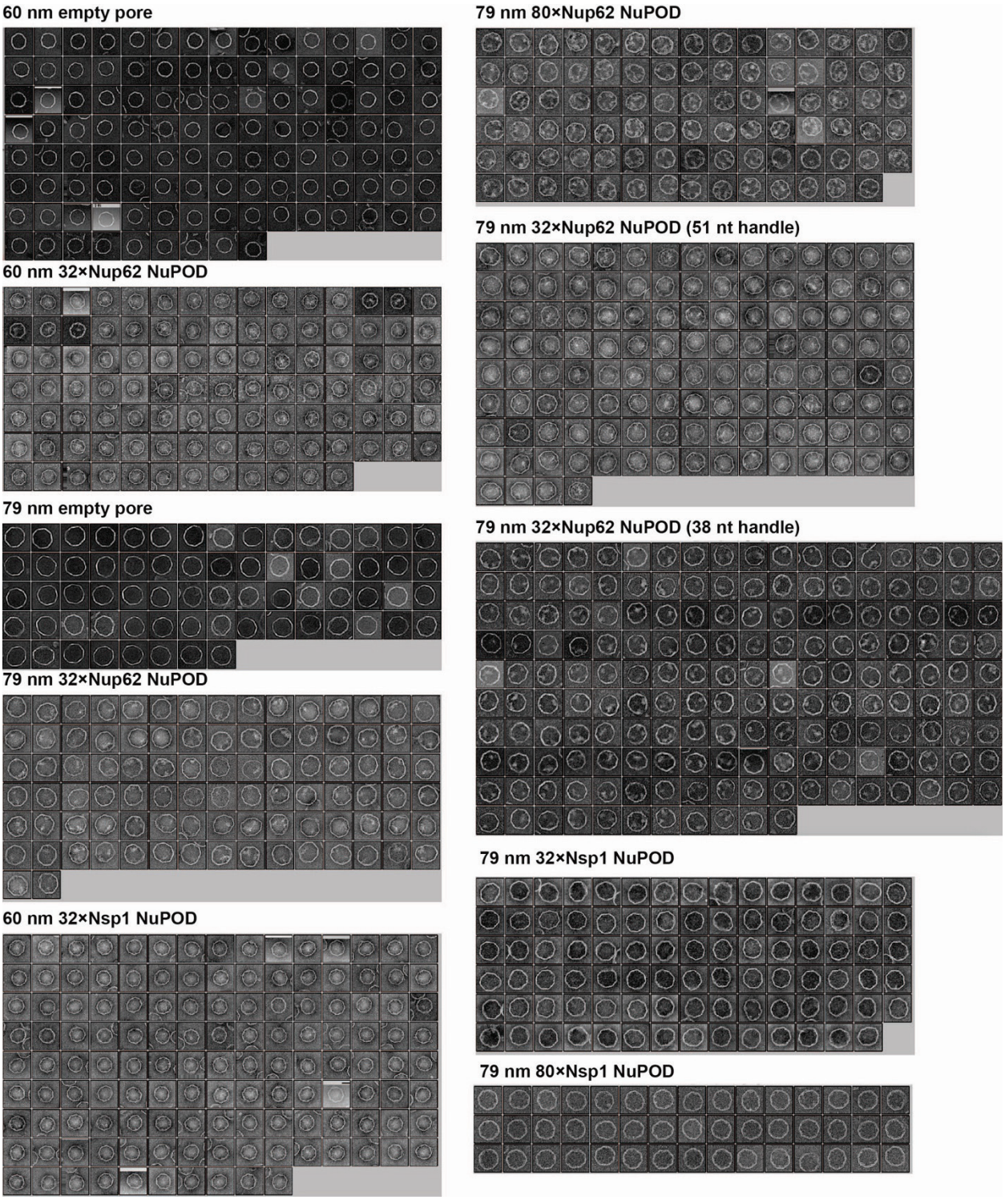

Figure S5. Negative-stain TEM image galleries of empty DNA nanopores and NuPODs.
The RELION 2D average and a few representative images of each sample are shown in **Figure 2** and **Figure S6**.

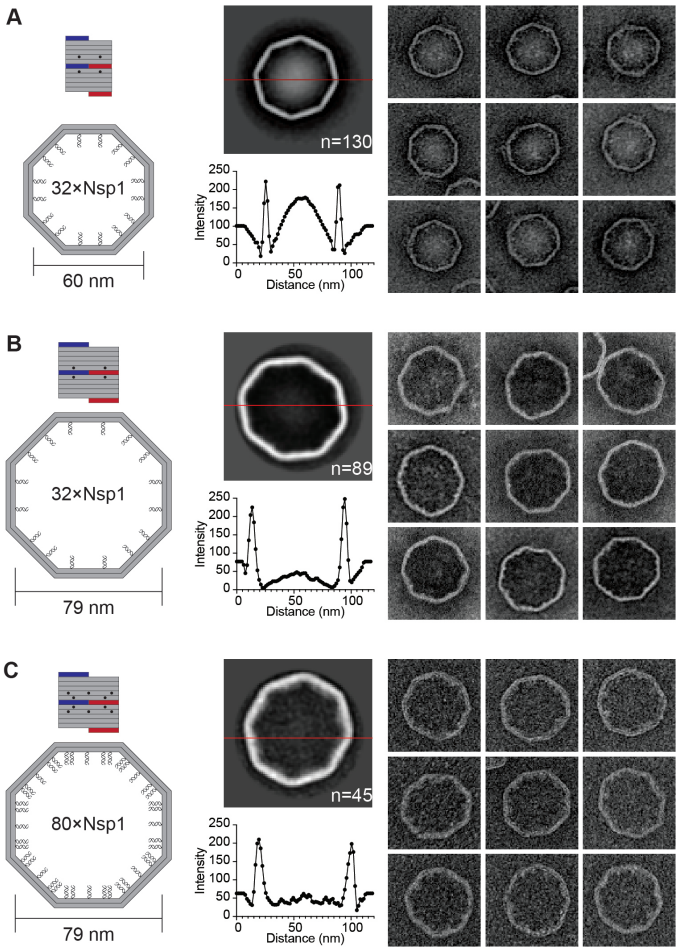

Figure S6. Morphology of Nsp1 inside NuPODs of different widths.
(A) 60-nm NuPOD with 32 copies of Nsp1. **(B)** 79-nm NuPOD with 32 copies of Nsp1. **(C)** 79-nm NuPOD with 80 copies of Nsp1. For each panel, left: schematics showing an interior face (top, nup-grafting handle positions denoted by black dots) and the top view (bottom, handle/anti-handle pairs shown as double helices) of a DNA channel; middle: class average negative-stain TEM image (top) and intensity profile across the center of the DNA channel (red line); right: representative TEM images of the DNA channel. All images are 120×120 nm^2.

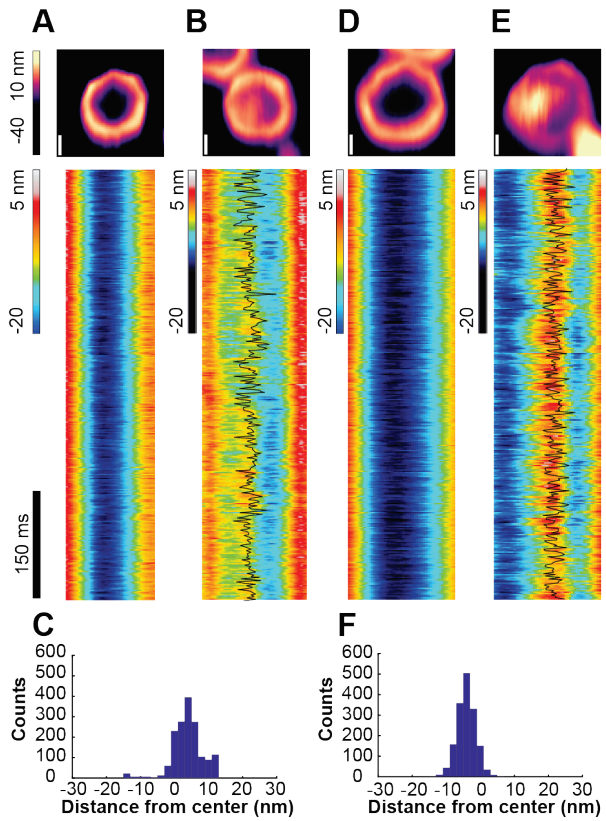

Figure S7. Protein dynamics inside Nup62 NuPODs with importin-β1.
(A) 60-nm Nup62 NuPOD with 10 nM importin-β1 (impβ). **(B)** 60-nm Nup62 NuPOD with 1 μM impβ. Top row: representative AFM images, scale bars: 20 nm; middle row: representative kymographs derived from HS-AFM line scans (1.875 ms/line), with movement tracking of the protein cluster overlaid (black line) for the 1 μM impβ condition. **(C)** A histogram summarizing the positions of the protein cluster in the 60-nm Nup62 NuPOD with 1 μM impβ. **(D)**–**(F)** are the same as **(A)**–**(C)**, except for the 79-nm NuPODs.

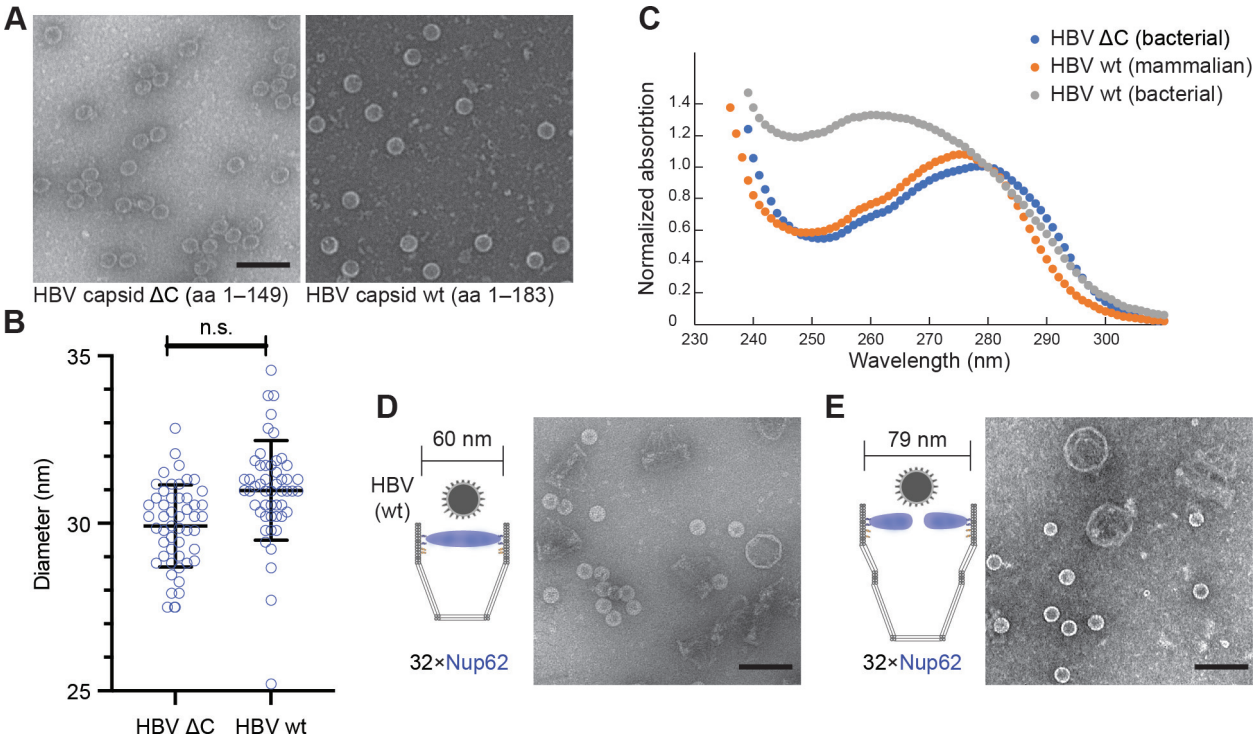

Figure S8. Characterization of HBV capsids.

(A) TEM images of capsids assembled from wild-type (wt) and C-terminus truncated (ΔC) HBc. Scale bar: 100 nm. **(B)** Measured diameters of HBV capsid wt (30.98 ± 1.73 nm, n=50) and ΔC mutant (29.92 ± 1.11 nm, n=50). P=0.1763 based on a two-tailed t-test; n.s.: not significant. **(C)** Absorption curves of HBV capsids normalized to OD_{280}. Nucleic acids in capsids assembled from E. coli expressed wt HBc are indicated by large OD_{260} (grey line). **(D)** HBV capsids (wt) mixed with 60-nm Nup62 NuPODs capped at one end. **(E)** HBV capsids (wt) mixed with 79-nm Nup62 NuPODs capped at one end. For **(D)** and **(E)**, a schematic of the binding experiment is shown next to a representative TEM image. Scale bar: 100 nm.

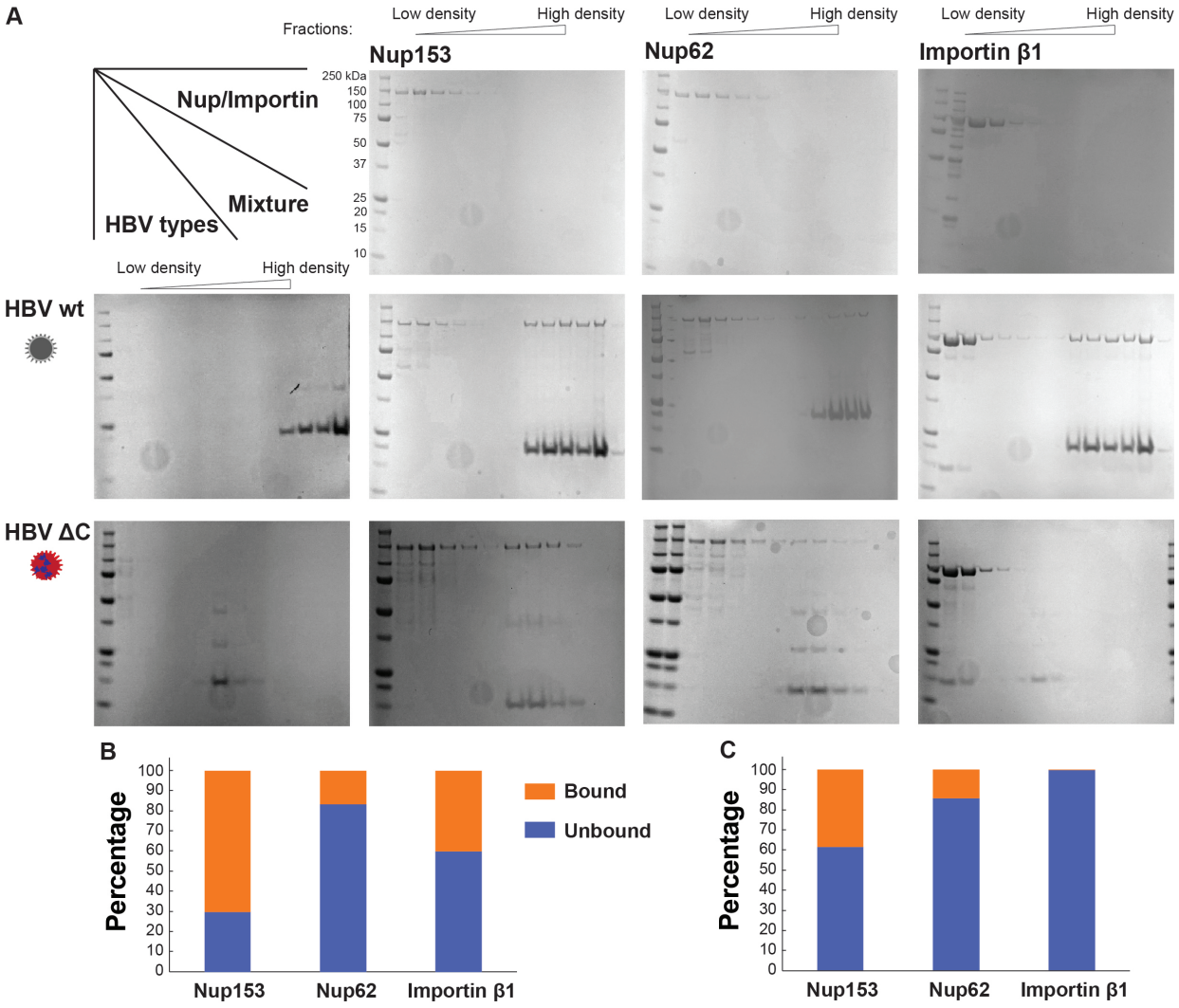

Figure S9. Comigration assays showing HBV capsid binding with nups and importin-β1.
(A) SDS-PAGE characterization of the fractions recovered from the comigration assay, in which nups or importin (1 μM) were mixed with capsids (~3 μM of HBc), loaded to the top of 15%–45% glycerol gradients, and spun at 48,000 rpm for 90 min. Lighter fractions are shown on the left. Gels in the top row contain pure nups and importins. Gels in the left column contain purified HBV capsids. The rest of gels contain capsids mixed with nup or importin, the contents of which are identified by the row/column headers. Capsid binding is indicated by the existence of nup or importin in the 4–5 heaviest fractions where capsids reside. **(B)** Band intensities measured from gels characterizing Nup153 (blue), Nup62 (orange) and importin-β1 (grey) binding to the wild-type (wt) HBV capsid, normalized to the total band intensity of the respective proteins across the whole gradient. **(C)** Same as (B), except for the HBV capsid with C-terminus deletion (ΔC).

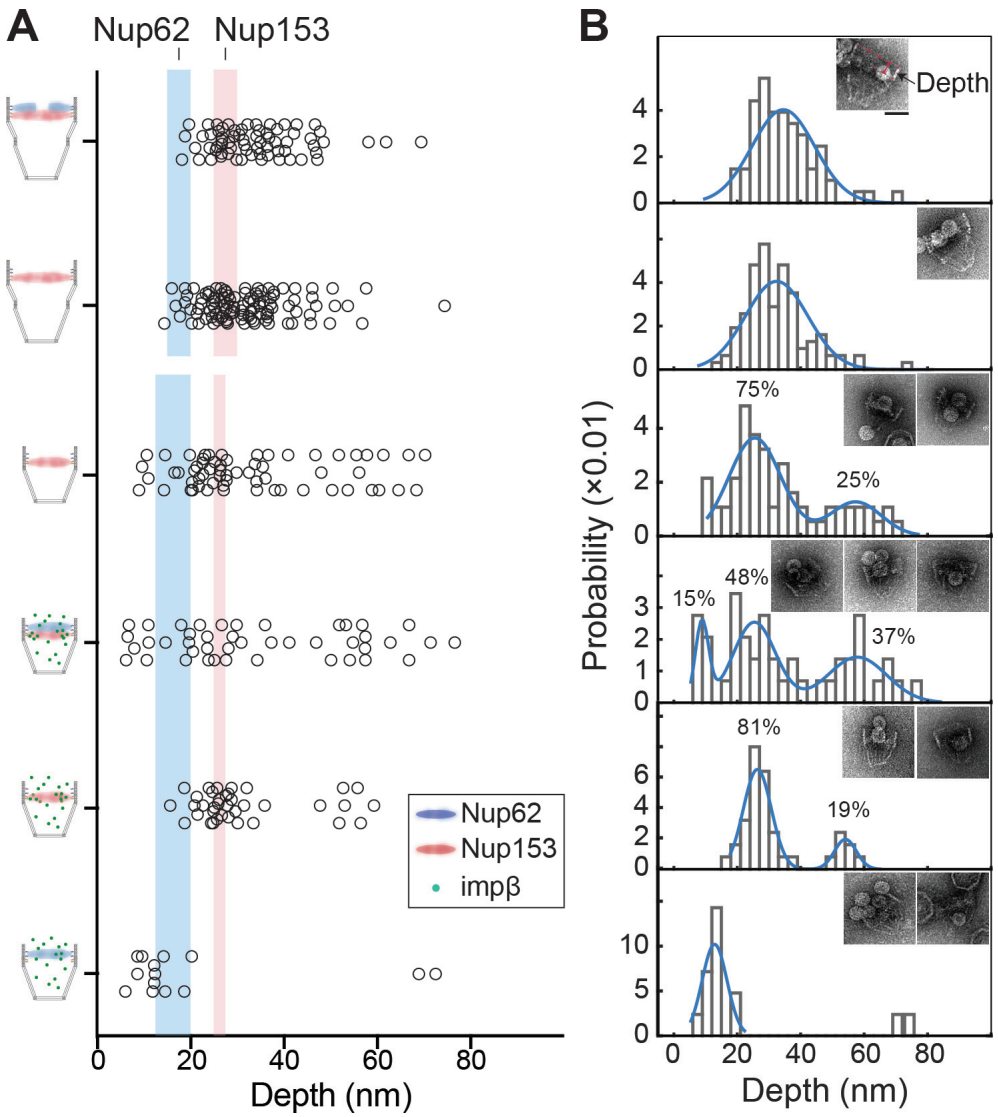

Figure S10. Depths of HBV capsid penetration into NuPODs.

(A) Scatter plot of the capsid penetration depths (from the center of capsids to the opening of NuPODs). Blue and red bands denote the anchoring positions of Nup62 and Nup153 in NuPODs, respectively. NuPOD schematics are shown on the left of the scatter plot. When presented, importin-β1 (impβ) concentration is 100 nM. **(B)** The capsid penetration depths plotted as histograms with Gaussian fit. When fitted using multiple Gaussian curves, the percentage and a representative TEM image of each population are shown. Scale bar: 50 nm. Number of NuPODs measured: 79-nm Nup62-Nup153 NuPODs (n=68); 79-nm Nup153 NuPODs (n=104); 60-nm Nup153 NuPODs (n=62); 60-nm Nup62-Nup153 NuPODs with impβ (n=43); 60-nm nup153 NuPODs with impβ (n=37); 60-nm Nup62 NuPODs with impβ (n=14).

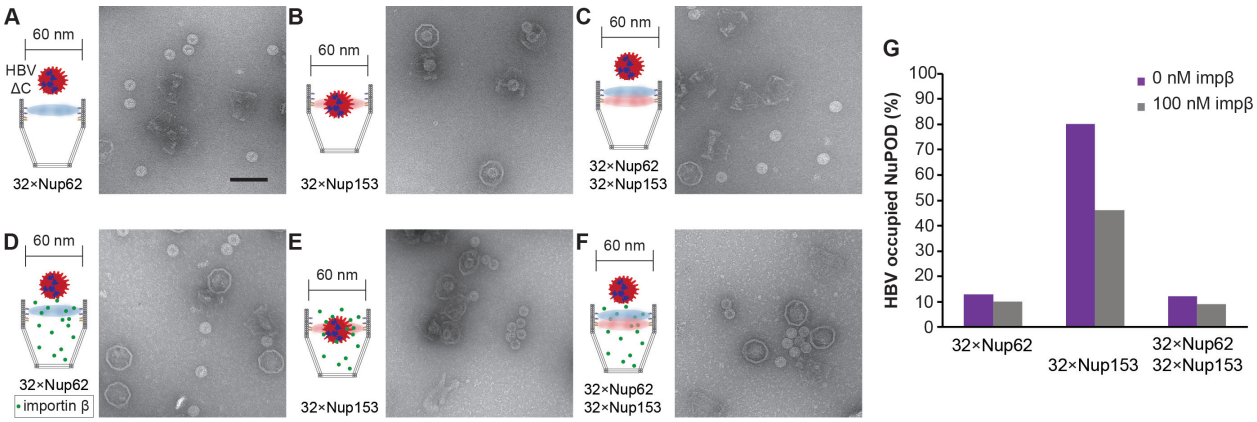

Figure S11. HBV capsids with C-terminus deletion (ΔC) interacting with NuPODs.

(A) $HBV^{\Delta C}$ capsids mixed with capped 60-nm Nup62 NuPODs. This experiment was repeated twice (technical replicates) with similar results. **(B)** $HBV^{\Delta C}$ capsids mixed with capped 60-nm Nup153 NuPODs. This experiment was repeated twice (technical replicates) with similar results. **(C)** $HBV^{\Delta C}$ capsids mixed with capped 60-nm Nup62-Nup153 NuPODs. **(D)**–**(F)** are the same as **(A)**–**(C)**, but in the presence of 100 nM importin-β1 (impβ). For **(A)**–**(F)**, schematic diagrams of the binding experiments are shown next to representative TEM images. Scale bar: 100 nm. **(G)** Percentages of NuPODs occupied by the $HBV^{\Delta C}$ capsids in experiments **(A)**–**(F)**. NuPODs counted in each experiment are (from left to right): 131, 299, 252, 454, 250 and 201.

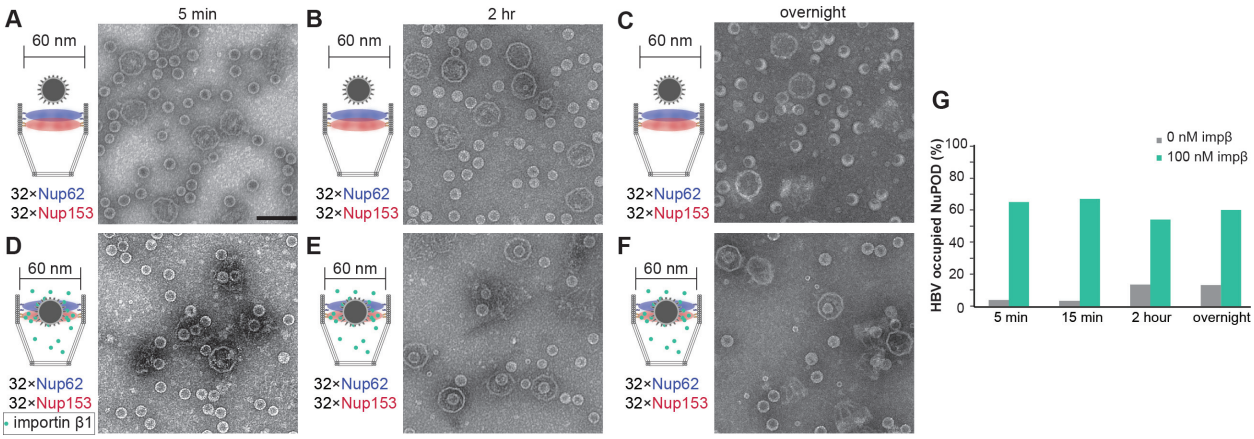

Figure S12. A time course study of HBV capsid interactions with NuPODs.

(A–C) HBV capsids mixed with capped 60-nm Nup62-Nup153 NuPODs in the absence of importin β1 (impβ) after 5 min **(A)**, 2 hour **(B)**, and overnight **(C)** incubation at room temperature. This experiment was repeated twice (technical replicates) with similar results. **(D–F)** HBV capsids mixed with capped 60-nm Nup62-Nup153 NuPODs in the presence of 100 nM importin-β1 (impβ) after 5 min **(D)**, 2 hour **(E)**, and overnight **(F)** incubation at room temperature. This experiment was repeated twice (technical replicates) with similar results. For **(A)**–**(F)**, schematic diagrams of the binding experiments are shown next to representative TEM images. Scale bar: 100 nm. **(G)** Percentages of NuPODs occupied by HBV capsids with (green) or without (grey) 100 nM impβ. NuPODs counted in each experiment (from left to right):402, 475, 279, 203, 462, 431, 320 and 410. Occupancies of Nup62-Nup153 NuPODs in the presence and absence of impβ with 15 min incubation time (**Figure 5D**) are shown here for comparison.

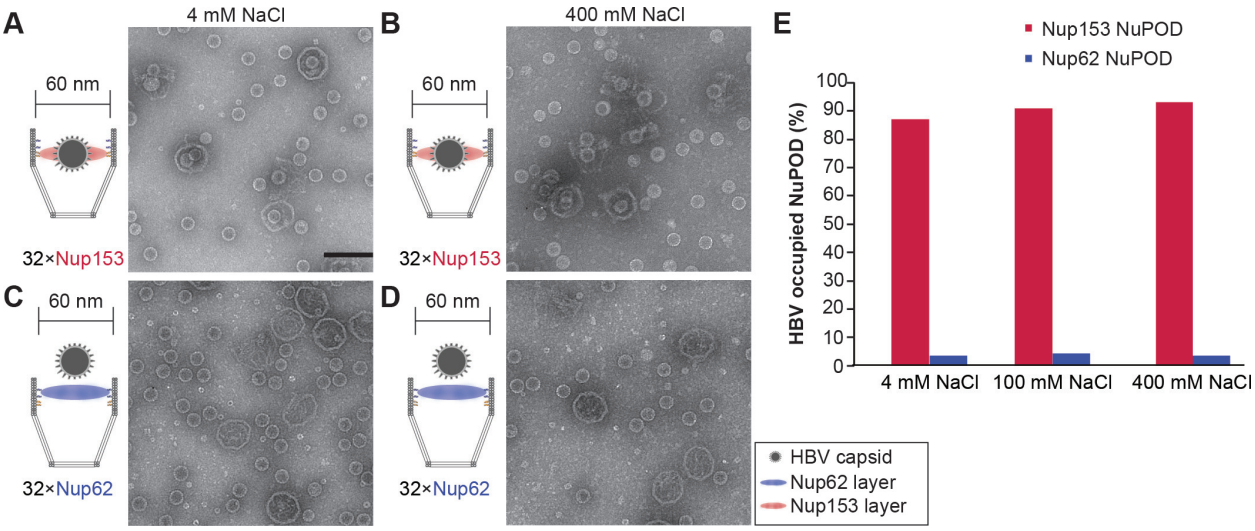

Figure S13. HBV capsid interactions with NuPODs in solutions with different ionic strength.
(A) HBV capsids mixed with capped 60-nm Nup153 NuPODs in buffer containing 4 mM NaCl. **(B)** HBV capsids mixed with capped 60-nm Nup153 NuPODs in buffer containing 400 mM NaCl. **(C)** HBV capsids mixed with capped 60-nm Nup62 NuPODs in buffer containing 4 mM NaCl. This experiment was repeated twice (technical replicates) with similar results. **(D)** HBV capsids mixed with capped 60-nm Nup62 NuPODs in buffer containing 400 mM NaCl. For **(A)**–**(D)**, schematic diagrams of the binding experiments are shown next to representative TEM images. Scale bar: 100 nm. All buffer solutions contain 1×TE (pH 8.0) and 15 mM $MgCl_2$. **(E)** Percentages of NuPODs occupied by HBV capsids in experiments **(A)**–**(D)**. NuPODs counted in each experiment are (from left to right): 237, 276, 168, 288, 280 and 276. Occupancies of Nup153 and Nup62 NuPODs in 100 mM NaCl (**Figure 5D**) are shown here for comparison.

Supplementary Movie Legends

Movie S1. AFM recording of 60-nm Nup62 NuPOD in the presence of 100 nM importin β1. The arrowhead tracks the movement of the central-plug-like structure. Scale bar: 10 nm.

Movie S2. AFM recording of 79-nm Nup62 NuPOD in the presence of 100 nM importin β1. The arrowhead tracks the movement of the central-plug-like structure. Scale bar: 10 nm.

Supplementary Data Legend

Data S1. DNA oligonucleotide sequences for assembling NuPODs.